

https://dspace.org/

Effects of a simulated slag phase on mixing and mass transfer rates in a creusot-loire uddeholm converter model

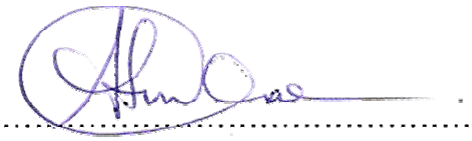
Chaendera, Admire

2006-10-31T10:38:14Z
http://hdl.handle.net/10539/1527

Downloaded from a DSpace repository. https://dspace.org/

DECLARATION

I declare that this dissertation is my own, unaided work. It is being submitted for the Degree of Master of Science in the University of the Witwatersrand, Johannesburg. It has not been submitted before for any degree or examination in any University.



Admire Chaendera

26 JAN 2006

Date

ACKNOWLEDGEMENTS

I would like thank everyone who was involved in the project. I greatly appreciate the support and guidance I received from my supervisor Prof R.H. Eric and Prof S. Küçükkaragoz. Valuable assistance was also received from Dr Akdogan and my fellow students. It has been a long journey but I leave Witwatersrand with happy memories. I want to thank everyone who made my stay pleasant. Many thanks go to the staff of the school of Chemical and Metallurgical Engineering. I was a pain in the neck sometimes but you were ever nice to me and willing to assist. My friends and family were with me all the way and I am grateful. This one is for you mum.

This work could not have been possible without financial support from Columbus Stainless Steel (Pty) Ltd.

ABSTRACT

An experimental study of the effects of a slag phase on mass transport in a one-fifth water model of a 100ton CLU-converter was conducted. The study was a follow up to earlier investigations conducted in the absence of a simulated slag phase. Kerosene (10% by volume) was used to represent the slag phase in the cold model experiments. The presence of a slag phase increased the mixing time of a tracer solution in the bath. The mixing time, defined at 99.66% bath homogeneity, was found to increase with bath height and a lowering gas flow rate. The functional relationship, $T_{mix} = 4.39Q^{-0.73}W^{0.24}H^{1.12}$, was established as expressing the effect of gas flow rate (Q), bath weight (W), and bath height (H) on the mixing time (T_{mix}). The mixing time increased by an average of 16.3% after slag inclusion. The mass transfer parameter $[(Re_{loc,r})^{0.25}(Re_t)^{0.32}]$ values obtained in the absence of a slag phase decreased by an average of 32.2% with slag inclusion. Calculated mass transfer coefficients increased with gas flow rate and a decrease in bath height. The relationship, $K \alpha Q^{0.08}$, showing derived mass transfer coefficient (K) dependence on the gas flow rate (Q) was established. The proportionality constant in the equation was observed to vary with bath height, gas flow rate and sample location. Contour maps representing variation of mass transfer coefficients in the bath regions were produced.

CONTENTS

		Page
DECLARATION		i
ACKNOWLEDGEMENTS		ii
ABSTRACT		iii
CONTENTS		iv
LIST OF FIGURES		vii
LIST OF TABLES		x
NOMENCLATURE		xi
1	**INTRODUCTION**	**1**
2	**LITERATURE REVIEW**	**4**
2.1	The CLU process	4
2.2	Previous studies on mass transport in the CLU-converter	6
2.3	Mass transport in the CLU-Converter	7
2.4	Physical Modelling	8
2.4.1	Method of determining gas flow rate in water model	11
2.4.2	Effect of temperature and pressure on gas flow rate	12
2.4.3	Calculation of the similarity criterion	14
2.5	Kinetics of reactions	16
2.6	The slag phase	17
2.6.1	Effect of slag phase on mixing time	18
2.7	Mixing in the gas stirred systems	19
2.8	Established correlations	22
2.8.1	Effect of specific energy input on mixing time	23
2.9	Water properties	24
2.10	Two-phase mass transfer	25
2.11	Factors affecting dissolution of additives	28

2.11.1 Turbulence and its effect on mass transfer 28
2.11.2 Determination of mass transfer parameters 29

3 EXPERIMENTAL MEASUREMENTS 31

3.1 Introduction 31
3.2 Experiments and sample preparation 32
3.3 Bath mixing intensity measurements 33
3.3.1 Establishing location of the probe and the dosing point 34
3.3.2 Mixing time measurements 35
3.4 Mass transfer experiments 36

4 RESULTS AND DISCUSSION 40

4.1 Establishing location of the probe and the dosing point 40
4.1.1 The Q-test 40
4.2 Mixing time measurements 44
4.2.1 Effects of gas flow rate 47
4.2.2 Effects of bath height 50
4.2.3 Establishing the mixing time correlation 52
4.3 Mass transfer experiments 60
4.3.1 Effect of gas flow rate on mass transfer rates 60
4.3.2 Effect of bath height on mass transfer rates 66
4.3.3 Mass transfer coefficient variation with gas injection rates 69
4.4 Mapping experiments 73
4.4.1 Effect of the slag phase and gas flow rate on mass transfer 80
4.5 Effect of the simulated slag phase on mixing time 87
4.5.1 Differences in the way the collected data was analysed 90
4.6 Comparison of mixing time and mass transfer rates 97
4.7 Scale up of model results to the industrial size vessel 98
4.8 Relating the full scale model to the actual vessel 100

5 CONCLUSION AND FUTURE WORK 102

6 REFERENCES 104

7 APPENDICES

Appendix 1 106
Appendix 2 107
Appendix 3 108
Appendix 4 109
Appendix 5 110
Appendix 6 111
Appendix 7 112
Appendix 8 124
Appendix 9 133
Appendix 10 136

LIST OF FIGURES

Figure		Page
3.1	The schematic representation of the 0.2-scale CLU-converter model	31
4.1	The general form of pH variation with time in the experiments as represented with results obtained using pure water at a bath height of 0.50m and a gas flow rate of 0.01m^3/s.	43
4.2	Effect of gas flow rate on the mixing time.	48
4.3	Effect of bath height on the mixing time.	51
4.4	Effect of specific stirring energy on mixing time in the model.	55
4.5	A comparison of the deviations of the estimates from the experimentally determined mixing time values.	59
4.6	Effect of gas flow rate on mass transfer coefficient at 0.4m water bath height.	61
4.7	Effect of gas flow rate on mass transfer coefficient at 0.5m water bath height.	64
4.8	Effect of gas flow rate on mass transfer coefficient at 0.65m water bath height.	66
4.9	Effect of bath height on mass transfer coefficient at a constant gas flow rate of 0.010m^3/s.	67
4.10	Effect of bath height on mass transfer coefficient at a constant gas flow rate of 0.0150m^3/s.	67
4.11	Effect of bath height on mass transfer coefficient at a constant gas flow rate of 0.023m^3/s.	68
4.12	Derived mass transfer coefficients *vs* gas flow rate in the J.K. Wright[8] 1kg apparatus.	72
4.13	The area represented on contour maps.	74
4.14	Contour and surface plots of mass transfer coefficient near the cone region of the bath at 0.01m^3/s gas flow rate.	75
4.15	Mass transfer coefficient variations in three regions at a gas flow rate of 0.01m^3/s.	77

Figure **Page**

4.16 Mass transfer coefficient variations in three regions at a gas flow rate of 0.015m^3/s 77

4.17 Mass transfer coefficient variations in three regions at a gas flow rate of 0.023m^3/s 79

4.18 Comparison of mass transfer coefficient values at a gas flow rate of 0.010m^3/s in the bottom region 80

4.19 Comparison of mass transfer coefficient values at a gas flow rate of 0.015m^3/s in the bottom region 81

4.20 Comparison of mass transfer coefficient values at a gas flow rate of 0.023m^3/s in the bottom region. 81

4.21 Comparison of mass transfer coefficient values at a gas flow rate of 0.010m^3/s near the cone region. 83

4.22 Comparison of mass transfer coefficient values at a gas flow rate of 0.015m^3/s near the cone region. 83

4.23 Comparison of mass transfer coefficient values at a gas flow rate of 0.023m^3/s near the cone region. 84

4.24 Comparison of mass transfer coefficient values at a gas flow rate of 0.010m^3/s near the water bath surface region. 86

4.25 Comparison of mass transfer coefficient values at a gas flow rate of 0.015m^3/s near the water bath surface region. 86

4.26 Comparison of mass transfer coefficient values at a gas flow rate of 0.023m^3/s near the water bath surface region. 87

4.27 Effect of the slag phase inclusion on the mixing time values predicted for model converter operations. 88

4.28 Mixing time variation with gas flow rate at a water bath height of 0.50m. 93

4.29 Mixing time variation with gas flow rate at a water bath height of 0.55m. 93

4.30 Mixing time variation with gas flow rate at a water bath height of 0.60m. 93

Figure **Page**

4.31 Mixing time variation with gas flow rate at a water bath height of 0.65m**.** 94

4.32 Mixing time variation with gas flow rate at a water bath height of 0.70m. 94

4.33 Mixing time variation with bath height at a gas flow rate of 0.010m^3/s. 94

4.34 Mixing time variation with bath height at a gas flow rate of 0.0127m^3/s. 95

4.35 Mixing time variation with bath height at a gas flow rate of 0.0150m^3/s. 95

4.36 Mixing time variation with bath height at a gas flow rate of 0.0183m^3/s. 95

4.37 Mixing time variation with bath height at a gas flow rate of 0.0212m^3/s. 96

4.38 Comparison of the mixing time and turbulence parameter variations with an increase in gas flow at a water bath height of 0.50m. 98

LIST OF TABLES

Table		Page
2.1	Process consumables in a typical CLU process[7].	5
2.2	Summary of physical properties of real system at 1600^{o}C.	11
2.3	Summary of physical properties of the cold model system.	11
2.4	Solubilities of benzoic acid in water.	26
4.1	Critical values of Q at the 90% confidence limit.	40
4.2	The mixing time values obtained at various gas flow rates and different arrangements of acid dosing and probe location points.	41
4.3	Mixing time results obtained at 0.0212m^3/s gas flow rate in the absence of a simulated slag phase.	45
4.4	Mixing time results obtained at 99.66% bath homogeneity in the presence of a simulated slag phase.	46
4.5	Energy considerations for the different conditions investigated.	53
4.6	Mixing time correlations for the investigated water bath heights.	54
4.7	Calculated values of the coefficients y and z.	58
4.8	The gas flow rate effect on different mass transfer properties at a water bath height of 0.4m.	60
4.9	The gas flow rate effect on different mass transfer properties at a bath height of 0.5m.	63
4.10	The gas flow rate effect on different mass transfer properties at a bath height of 0.65m.	65
4.11	Mass transfer coefficients in the model converter vessel under conditions of varying bath height.	70
4.12	Turbulence parameters calculated from the mapping experiments.	73
4.13	Mixing time values obtained in the presence of a slag phase.	92
4.14	Mixing time values obtained in the absence of a slag phase[2,3].	92
4.15	A comparison of the T_{mix} values obtained with and without slag.	96
4.16	Gas flow rates adopted in the model systems and those used in the actual operation.	100

NOMENCLATURE

N_{Fr}	dimensionless, modified Froude number
ρ_g	gas density (kg/m^3)
ρ_l	liquid density (kg/m^3)
g	acceleration due to gravity (m/s^2)
d	diameter of the nozzle (m)
P	pressure of the gas (atm)
M	molecular weight of the gas (g mol^{-1})
I_t	time (s)
U_g	gas flow rate in real system (m^3/s)
U_{air}	gas flow rate in the full size water model (m^3/s)
$U_{g,nom}$	nominal velocity of the gas in the nozzle(m/s)
A	cross sectional area (m^2)
Q_m	gas flowrate operating in the water model of reduced size (m^3/s)
Q_{fs}	gas flowrate operating in the water model of full size (m^3/s)
λ	ratio of reduction.
μ	viscosity of a liquid (cP)
σ	surface tension between two liquids (dyne/cm)
T_{mix}	mixing time (s)
W	bath weight (tons)
v	velocity of the gas in the nozzle (m/ s)
KE	kinetic energy (J)
P_s	Stirring power (J/s)
$\dot{m}$	mass of the purging gas per unit time (kg/s)
ρ	density of the purging gas per unit time (g/m^3)
M	molecular weight of the purging gas (kg/mol)
R	ideal gas constant (J mol^{-1} K^{-1})
V	volume of the purging gas (m^3)
u	mean plume velocity (m/s)
L	liquid depth (m)
r	radius of vessel (m)

K	mass transfer rate constant (m/s)
b,m,y,z	experimentally determined coefficients
E_b	stirring energy density due to buoyancy (W/ton)
Q	gas flow rate (N m^3/s)
H	bath height/depth (m)
H_{wb}	water bath height (m)
E_k	stirring energy density (W/ton)
E_t	total mixing energy density (W/ton)
a	experimentally determined constant
n	gas stirring factor of gas flow rate
pH_{cs}	temperature compensated 'stable' pH value
pH_i	initial pH value of the solution before acid dosing
$pH_{99.66\%}$	pH value when the bath had reached 99.66% homogeneity level
D_o	mass diffusion coefficient
Sh	Sherwood number
Re	Reynolds number
$Re_{loc,r}$	local nominal Reynolds number
Re_t	local turbulent Reynolds number
Sc	Schmidt number
C^*_s	saturation concentration of acid (kg/m^3)
C_s	bulk concentration (kg/m^3)
μ	axial component of velocity (m/s)
v	radial component of velocity (m/s)
u_o	nominal gas velocity (m/s)
L_{mod}	the depth of liquid in model (m)
L_{fs}	depth of liquid in full-scale model (m)
T	temperature (K)